Spectral investigation of Sm^{3+}/Yb^{3+}co-doped sodium tellurite glass

Fakhra Nawaz[1,2], Md. Rahim Sahar[1*], S. K. Ghoshal[1], Raja, J. Amjad[1], M. R. Dousti[1], and Asmahani Awang[1]

[1]*Advanced Optical Material Research Group, Department of Physics, Faculty of Science, Universiti Teknologi Malaysia, 81310 Skudai, Johor, Malaysia*

[2]*Experimental Physics Labs, National Center for Physics, Quad-i-Azam University, Islamabad, Pakistan*

[*]*Corresponding author: mrahim057@gmail.com*

Received January 17, 2013; accepted March 29, 2013; posted online May 31, 2013

Sm^{3+}/Yb^{3+} co-doped tellurite glasses are prepared by melt-quenching technique. The density of the glasses varies between 4.65 and 4.84 g/cm^3. The optical absorption spectra consist of eight bands in the wavelength range of 350–2 000 nm, which correspond to the transitions from ground level $^6H_{5/2}$ to the various excited states of the Sm^{3+} ion. Energy band gaps vary in the range of 2.73–2.91 eV, and the Urbach energy ranges from 0.21 to 0.27. Emission spectra exhibit four peaks originating from the $^4G_{5/2}$ energy level centered at 576, 613, 657, and 718 nm. Quenches in emission bands may be due to the energy transfer from the Sm^{3+} to Yb^{3+} ions.

OCIS codes: 160.2750, 160.4760, 140.0140.
doi: 10.3788/COL201311.061605.

Tellurite glass is a well-known and interesting material because of its linear and nonlinear applications in optics, as well as its outstanding features, such as low melting temperature, slow crystallization rate, good thermal and chemical stability, low cut-off phonon energy, and high refractive index[1,2]. Among the rare earth (RE) ions, Sm^{3+} is the most studied even in high-phonon energy glasses because of the large energy difference (7 000 cm^{-1}) between the metastable level $^4G_{5/2}$ and its next lower lying level $^6F_{11/2}$[3,4]. Therefore, the phonon energy of the glass is not a critical issue for red and green emissions. Research on the optical properties of Sm^{3+}-doped glasses has elicited considerable attention because of their technological applications. The Sm^{3+} ion also exhibits broad photoluminescence bands originating from $^4G_{5/2}\rightarrow{}^6H_J$ (J= 5/2, 7/2, 9/2, and 11/2) transitions in any host glass. Sm^{3+}-doped glasses are important for the development of solid-state lasers, optical amplifiers, temperature sensors, and light-emitting diodes (LEDs)[5–7]. Studies have demonstrated that two or more RE; ions can be added to enhance the optical properties by energy transfer process[8,9]. The energy levels of the Sm^{3+} ions for optical amplification require a high pump rate to achieve population inversion. However, the low absorption cross-section of Sm^{3+} ions limits pump efficiency. Yb^{3+} ions exhibit a large absorption cross-section and broad absorption band between 800 and 1 100 nm[10]. Furthermore, the large spectral overlap between Yb^{3+}:$^2F_{7/2}\rightarrow{}^2F_{5/2}$ and Sm^{3+} absorption $^6H_{5/2}\rightarrow{}^6F_{11/2}$ results in an efficient resonant energy transfer (ET) from Yb^{3+} to Sm^{3+} in a co-doped system.

The optical absorption spectrum of crystalline and amorphous solids in the ultraviolet (UV) region provides essential information about band structure and band gap energy. The characteristics of atomic vibrations can be obtained by measuring the absorption spectra in the lower energy region[11]. Refractive index and optical band gap energy are important properties in optical glasses. Many reports have determined the relation between refractive index and composition of the transparent system[12]. Amjad *et al.*[13] studied some of the physical and optical properties of samarium-doped zinc–lead–phosphate glasses. In their work, the attenuation in the refractive index is attributed to the variation in non-bridging oxygen (NBO) with Sm^{3+} ion concentration.

The purpose of this letter is to synthesize Sm^{3+}-doped sodium tellurite glasses co-doped with various Yb^{3+} concentrations. This research aims to study the absorption properties and understand the ET mechanism in Sm^{3+} and Yb^{3+} ions. All measured or evaluated results are compared with a Sm^{3+} single-doped tellurite glass sample.

Glasses with composition (80-x)TeO_2-20Na_2O-0.5Sm_2O_3–$x$$Yb_2O_3$ (where $0\leqslant x\leqslant$2.0 mol%) were prepared using melt-quenching technique. All chemical ingredients were weighed according to calculated quantities and mixed using a milling machine to obtain a homogenous mixture. The mixture was then melted at 850 °C in an alumina crucible for 45 min. Then, the melted mixture was quickly quenched between two preheated brass molds and annealed at 250 °C for 3 h to eliminate mechanical and thermal stresses. The X-ray diffraction (XRD) pattern of sodium tellurite glasses were recorded in the range of $0^\circ\leqslant 2\theta\leqslant 60^\circ$ to examine the amorphous nature of the samples. UV–visible (Vis)–near infrared (NIR) optical absorption measurements were performed in the spectral region from 350 to 2 000 nm at room temperature using a scanning spectrophotometer

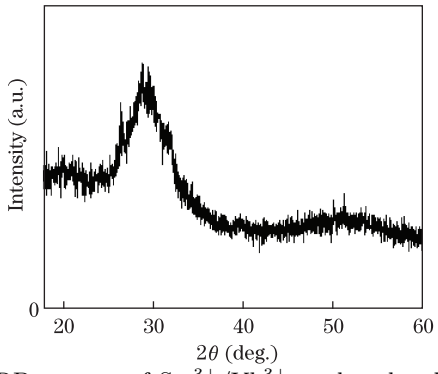

Fig. 1. XRD pattern of Sm^{3+}/Yb^{3+} co-doped sodium tellurite glass.

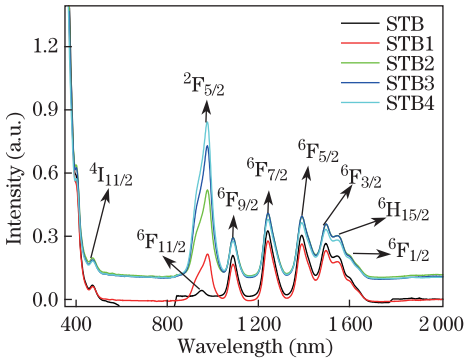

Fig. 2. (Color online) Optical absorption spectra for STB–STB4 glasses.

(Schimadzu UV-3101PC, Kyoto, Japan). Photoluminescence spectra were recorded in the range of 400–750 nm using a luminescence spectrometer (LS 55, PerkinElmer, UK) at 406-nm excitation wavelength.

The XRD spectra of all the prepared sodium tellurite glasses show that the samples similarly display an amorphous nature. Figure 1 shows the XRD spectra of sample STB2 with 0.5 mol% Sm_2O_3 and 1.0 mol% Yb_2O_3. The absence of a sharp crystalline peak indicates the amorphous nature of the glasses. The density of the glasses were measured by Archimedes method using ionized water with a density of 0.997 g/cm^3 as the immersion liquid at room temperature (25 °C). The corresponding molar volume is calculated using the relation $V_m = M/\rho$, where M and ρ are the molecular weight and the density of the sample, respectively. The addition of Yb_2O_3 into the Sm^{3+}-doped sodium tellurite glass increases the density, possibly because of the heavier molar weight of Yb_2O_3 (394.1 g· mol^{-1}) with respect to TeO_2 (159.6 g · mol^{-1}). The molar volume of glasses decreases with the increase in Yb_2O_3 content, which is consistent with the increasing rigidity and compactness of the glass samples.

Figure 2 presents the UV-Vis-NIR spectra of all the prepared glass samples. The spectra consist of eight peaks, which are assigned to the transitions, namely, $^6H_{5/2} \rightarrow {}^4I_{11/2}, {}^6F_{11/2}, {}^6F_{9/2}, {}^6F_{7/2}, {}^6F_{5/2}, {}^6F_{3/2}, {}^6H_{15/2}$, and $^6F_{1/2}$. The intense and broad absorption of STB1, STB2, STB3, and STB4 glasses in the wavelength region of 870–1 040 nm is attributed to the large contribution of the absorption from the $^2F_{7/2} \rightarrow {}^2F_{5/2}$ transition of Yb^{3+}. All the transitions originated from the electric dipole contribution ($\Delta J \leqslant 6$), and the corresponding assignments were according to Babu *et al.*[14]. The absorption bands in the Vis region have low intensity because they are spin-forbidden. By contrast, the bands located in the NIR region are more intense and sharp because of the effective shielding of the 4f electron by the filled 5s and 5p shells[15].

Specific transitions of RE ions are very sensitive to the environment of the ion; these transitions are called hypersensitive transitions. These hypersensitive transitions obey the selection rules: $|\Delta S| = 0$, $|\Delta L| \leqslant 2$, and $|\Delta J| \leqslant 2$[16]. The $^6H_{5/2} \rightarrow {}^6F_{7/2}$ transition of Sm^{3+} ions is a hypersensitive transition and is more intense compared with other transitions. Figure 2 shows that the intensities of all absorption bands are slightly affected by the addition of the Yb^{3+} ion. However, the broad absorption peak at the range of 870–1 040 nm is highly affected by Yb^{3+}.

The absorption due to the band-to-band transition in amorphous materials determines the optical band gap. Generally, such absorption bands are used to explore the electronic band structure of crystalline and non-crystalline materials. The band gap is normally interpreted by Davis *et al.*[15] theory

$$\alpha = \frac{B(h\nu - E_{\text{opt}})^r}{h\nu}, \tag{1}$$

where B is a constant; α is the absorption coefficient; E_{opt} is the optical band gap of the material; $h\nu$ is the photon energy; r is the index, which can be 1/2, 2, 3/2, and 3 depending on the interband electronic transition[17]. Figure 3 shows the typical plot of $(h\nu\alpha)^{1/2}$ versus $(h\nu)$ for indirect transition in Sm^{3+}/Yb^{3+} co-doped sodium tellurite glasses.

At a particular temperature, a band tailing of density of the states in amorphous materials at the absorption edge can be defined by the empirical relation proposed by Urbach[18]

$$\ln(\alpha) = C + \frac{h\nu}{\Delta E}, \tag{2}$$

where C is a constant and ΔE is the Urbach energy derived by the inverse of the slope of the $\ln(\alpha)$ versus $h\nu$ plot. The Urbach energy was used to determine the degree of disorder in the amorphous and crystalline materials. The materials with higher Urbach energy have higher tendency for converting weak bonds to defects.

The band gap ranges from 2.73 to 2.91 eV, and the Urbach energy ranges from 0.21 to 0.27 eV. The energy band gap (E_{opt}) and Urbach energy (ΔE) of all the

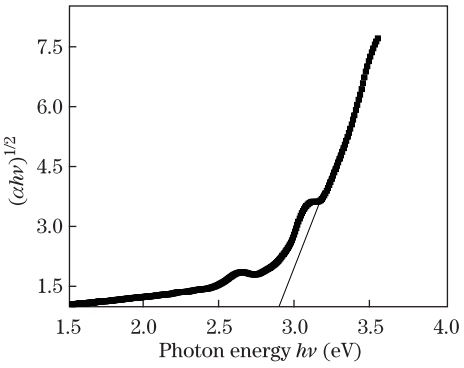

Fig. 3. Typical plot of $(h\nu\alpha)^{1/2}$ versus $h\nu$ in Sm^{3+}/Yb^{3+} co-doped sodium tellurite glass.

Table 1. Physical and Optical Properties of the Prepared Glasses

Sample Code	Yb_2O_3 (mol%)	Sm_2O_3+NaO (mol%)	TeO_2 (mol%)	ρ (g/cm^3)	V_m (cm$^3\cdot$ mol^{-1})	n	R_m (cm^{-3})	R (%)	E_{opt} (eV)	ΔE (eV)
STB	0	0.5+20	79.5	4.65	30.32	2.422	18.756	10.341	2.91	0.21
STB1	0.5	0.5+20	79.0	4.64	30.28	2.474	19.094	10.584	2.73	0.27
STB2	1.0	0.5+20	78.5	4.74	30.24	2.447	18.887	10.588	2.82	0.25
STB3	1.5	0.5+20	78.0	4.79	30.17	2.442	18.804	10.538	2.84	0.24
STB4	2.0	0.5+20	77.5	4.84	30.08	2.439	18.727	10.509	2.85	0.23

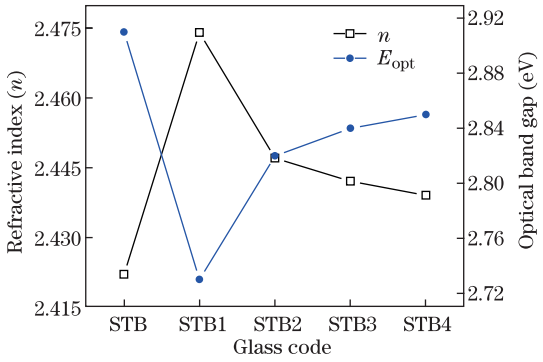

Fig. 4. Yb_2O_3 concentration-dependent variation in refractive index and band gap.

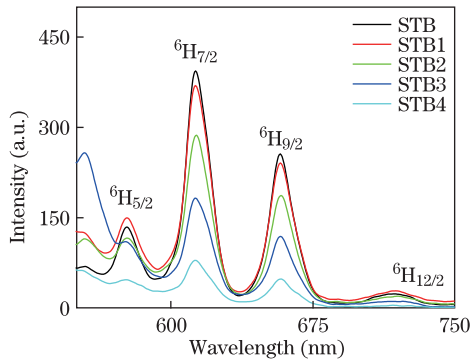

Fig. 5. (Color online) Emission spectra Sm^{3+}/Yb^{3+} co-doped sodium tellurite glass under 406-nm excitation wavelength.

studied glasses are listed in Table 1. The introduction of the Yb^{3+} ion up to 0.5 mol% in the Sm^{3+}-doped glasses leads to a decrease in band gap energy, and further addition of Yb_2O_3 in the Sm^{3+}-doped glasses results in a slight increase in optical band gap. This attenuation in band gap energy is due to the structural changes occurring in the glass network with the introduction of Yb_2O_3. Similar results were obtained by Yousef *et al.*[19], who attributed the decrease in the band gap to the increase in the number of NBOs. Generally, the position of the absorption edge depends on the strength of the oxygen bond in the glass formation network. Urbach energy is also a factor used for measuring the disorder of the materials. The addition of Yb_2O_3 increases the disorder in the glass, as revealed by the increasing values of the Urbach energy.

The refractive index of the glass series (n) is calculated from the relation proposed by Dimitrov *et al.*[16]

$$\frac{n^2-1}{n^2+2} = 1 - \sqrt{\frac{E_{opt}}{20}}. \tag{3}$$

The molar refractivity (R_M) and reflection loss (R%) were calculated using

$$R_M = V_M \frac{n^2-1}{n^2+2}, \tag{4}$$

$$R(\%) = \left(\frac{n-1}{n+2}\right)^2 \cdot 100. \tag{5}$$

Measured and calculated values of densities, molar volume, refractive indices, molar refractivity, and reflection loss, along with the composition of all studied glasses, are listed in Table 1. The variation in the refractive index and band gap with Yb_2O_3 content in the Sm^{3+}-doped glasses is illustrated in Fig. 4. The trend of refractive index changes is exactly opposite that of the band gap energy, as indicated by Eq. (3). Refractive index values highly depend on the polarizability and number of NBOs. The decrease in the refractive index after the addition of 0.5 mol% of Yb^{3+} in the Sm^{3+}-doped glasses is ascribed to the decrease in NBOs, which possess high polarizability. Therefore, refractive index can be altered by co-doping glasses with two different types of RE; ons or modifiers. The changes in the refractive index and band gap energy of the STB1 to STB4 are opposite those of STB to STB1. This variation in the band gap and refractive index of these glasses is attributed to the variation in the number of NBOs.

Photoluminescence spectra of the glass samples at 406-nm excitation wavelength are shown in Fig. 5. Four emission peaks at 576, 613, 657, and 718 nm originating from the transitions of the $^4G_{5/2}$ excited state to the $^6H_{5/2}$, $^6H_{7/2}$, $^6H_{9/2}$, and $^6H_{11/2}$ lower levels are observed.

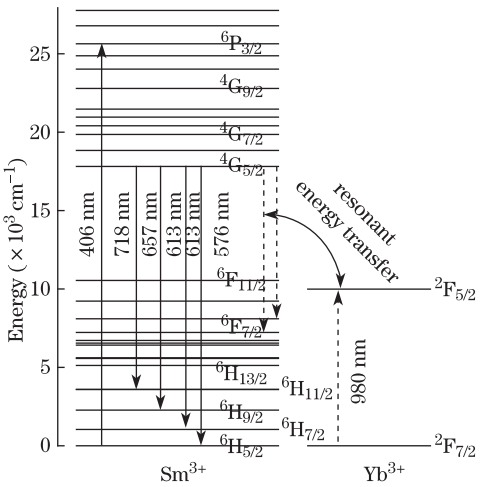

Fig. 6. Energy level diagram of the Sm^{3+} ion in the vicinity of the Yb^{3+} ion.

The $^4G_{5/2} \rightarrow {}^6H_{5/2}$ and $^6H_{7/2}$ transitions are electric and magnetic dipoles obeying the selection rule $\Delta J = 0, \pm 1$.

The other two transitions, namely, $^4G_{5/2} \rightarrow {}^6H_{9/2}$ and $^6H_{11/2}$, are purely electric dipoles in nature ($\Delta J < 6$). The intensity of all emission bands decreases with the increase in Yb^{3+} concentration.

The reduction in luminescence is due to the increase in non-radiative resonant ET mechanism from Sm^{3+} ions to neighboring Yb^{3+} ions as

$$^4G_{5/2} \rightarrow {}^6H_{9/2}(Sm^{3+}){:}^2F_{7/2} \rightarrow {}^2F_{5/2}(Yb^{3+}).$$

This non-radiative ET between dual RE ions is important for applications in sensitizing solid-state lasers, infrared quantum counters, and infrared to Vis convertors[20,21]. The radiative and non-radiative emissions of the different energy levels and resonant ET are illustrated in a partial energy level diagram in Fig. 6.

In conclusion, the optical properties of Sm^{3+}/Yb^{3+} co-doped sodium tellurite glasses are investigated. A series of Sm^{3+}-doped glasses with various Yb^{3+} concentrations are prepared by melt-quenching method and characterized by spectroscopic techniques. The density and volume of glasses range from 4.65 to 4.84 g/cm^3 and 30.32 to 30.08 cm$^3\cdot$ mol^{-1}, respectively. The absorption spectra consist of eight absorption bands assigned to the transitions $^6H_{5/2} \rightarrow {}^4I_{11/2}, {}^6F_{11/2}, {}^6F_{9/2}, {}^6F_{7/2}, {}^6F_{5/2}, {}^6F_{3/2}, {}^6H_{15/2}$, and $^6F_{1/2}$. The intense and broad absorption in the wavelength region of 870–1 040 nm is attributed to the absorption from the $Yb^{3+}{}^2F_{7/2} \rightarrow {}^2F_{5/2}$ transition. The band gaps of these glasses increase after the addition of 0.5 mol% of Yb^{3+}. The refractive index follows the opposite trend. All these attenuations are due to the decrease in the number of NBOs. Urbach energy varies between 0.21 and 0.27 eV. Photoluminescence spectra show four emission peaks at 576, 613, 657, and 718 nm at 406-nm excitation wavelength. The intensities of all the peaks are quenched with the increase in Yb^{3+} concentration, which is attributed to the resonant ET from the Sm^{3+} ion to the Yb^{3+} ion.

The authors acknowledge the financial support from the Research Management Centre, University Technology Malaysia (RMC, UTM) through the research grants (VOTE ERGS 4L032 and 07J80, MoHE). F. Nawaz extends his gratitude to the financial support by UTM through the International Doctoral Fellowship (UTM.J.10.01/13.14/1/128).

References

1. G. V. Prakash, D. N. Rao, and A. K. Bhatnagar, Solid State Commun. **119,** 39 (2001).
2. D. He, J. Zhang, G. Wang, Z. Duan, S. Dai, and L. Hu, Chin. Opt. Lett. **4,** 39 (2006).
3. M. C. Fearries, P. R. Morkel, and J. E. Townsend, Electron. Lett. **24,** 709 (1988).
4. G. Turky and M. Davy, Mater. Chem. Phys. **77,** 48 (2002).
5. A. Agarwal, I. Pal, S. Sanghi, and M. P. Aggarwal, Opt. Mater. **32,** 339 (2009).
6. Y. K. Sharma, S. S. L. Surana, and R. K. Singh, J. Rare Earths **27,** 773 (2009).
7. G. Tang, H. Xiong, W. Chen, and L. Luo, J. Non-Cryst. Solids. **357,** 2463 (2011).
8. J. Yang, L. Wen, S. Dai, L. Hu, and Z. Jiang, Chin. Phys. Lett. **1,** 611 (2003).
9. G. Lakshminarayana , R. Yang, J. R. Qiu, M. G. Brik , G. A. Kumar, and I. V. Kityk, J. Phys. D Appl. Phys. **42,** 015414 (2009).
10. X. Zou and H. Toratani, J. Phys. Rev. B **52,** 15889 (1995).
11. M. I. AbdEl-Ati and A. A. Higazy, J. Mater. Sci. **35,** 6175 (2000).
12. R. El-Mallawany, J. Appl. Phys. **72,** 1774 (1992).
13. R. J. Amjad, M. R. Sahar, S. K. Ghoshal, M. R. Dousti, S. Riaz, and B. A. Tahir, Chin. Phys. Lett. **29,** 087304 (2012).
14. A. M. Babu, B. C. Jamalaiah, T. Sasikala, S. A. Saleem, and L. R. Moorthy, J. Alloys Compounds **509,** 4743 (2011).
15. N. F. Mott and E. A. Davis, Philos. Mag. **22,** 903 (1979).
16. V. Dimitrov and S. Sakka, J. Appl. Phys. **79,** 1736 (1996).
17. S. K. J. Al-Ani and A. A. Higazy, J. Mater. Sci. **26,** 3670 (1991).
18. F. Urbach, Phys. Rev. **92,** 1324 (1953).
19. E. S. Yousef, A. El-Adawi, N. El Koshkhany, and E. R. Shaaban, J. Phys. Chem. Solids **67,** 1649 (2006).
20. S. Fuchi and Y. Takeda, Phys. Status Solidi C **8,** 2653 (2011).
21. S. Guan, Y. Tian, Y. Guo, L. Hu, and J. Zhang, Chin. Phys. Lett. **10,** 071603 (2012).